British Journal of Pharmacology (2008) 153, 1203–1213

0007–1188/08 $30.00
www.brjpharmacol.org

RESEARCH PAPER

Palmatine, a protoberberine alkaloid, inhibits both Ca^{2+}- and cAMP-activated Cl^- secretion in isolated rat distal colon

DZ Wu[1,2], JY Yuan[1], HL Shi[1] and ZB Hu[1]

[1]*Laboratory of Pharmacology, Institute of Chinese Materia Medica, Shanghai University of TCM, Shanghai, PR China and* [2]*E-Institute of TCM Internal Medicine, Shanghai Municipal Education Commission, Shanghai, PR China*

Background and purpose: The protoberberine alkaloid berberine has been reported to inhibit colonic Cl^- secretion. However, it is not known if other protoberberine alkaloids share these effects. We have therefore selected another protoberberine alkaloid, palmatine, to assess its effects on active ion transport across rat colonic epithelium.
Experimental approach: Rat colonic mucosa was mounted in Ussing chambers and short circuit current (I_{SC}), apical Cl^- current and basolateral K^+ current were recorded. Intracellular cAMP content was determined by an enzyme immunoassay. Intracellular Ca^{2+} concentration was measured with Fura-2 AM.
Key results: Palmatine inhibited carbachol-induced Ca^{2+}-activated Cl^- secretion and the carbachol-induced increase of intracellular Ca^{2+} concentration. Palmatine also inhibited cAMP-activated Cl^- secretion induced by prostaglandin E_2 (PGE_2) or forskolin. Palmatine prevented the elevation of intracellular cAMP by forskolin. Determination of apical Cl^- currents showed that palmatine suppressed the forskolin-stimulated, apical cAMP-activated Cl^- current but not the carbachol-stimulated apical Ca^{2+}-activated Cl^- current. Following permeabilization of apical membranes with nystatin, we found that palmatine inhibited a carbachol-stimulated basolateral K^+ current that was sensitive to charybdotoxin and resistant to chromanol 293B. However, the forskolin-stimulated basolateral K^+ current inhibited by palmatine was specifically blocked by chromanol 293B and not by charybdotoxin.
Conclusions and implications: Palmatine attenuated Ca^{2+}-activated Cl^- secretion through inhibiting basolateral charybdotoxin-sensitive, SK4 K^+ channels, whereas it inhibited cAMP-activated Cl^- secretion by inhibiting apical CFTR Cl^- channels and basolateral chromanol 293B-sensitive, KvLQT1 K^+ channels.
British Journal of Pharmacology (2008) **153,** 1203–1231; doi:10.1038/sj.bjp.0707684; published online 21 January 2008

Keywords: chloride secretion; colonic mucosa; palmatine; short circuit current; ion currents; cyclic adenosine monophosphate; intracellular calcium concentration

Abbreviations: 293B, chromanol 293B; 8-bromo-cAMP, 8-bromoadenosine 3′,5′-cyclic monophosphate; $[Ca^{2+}]_i$, intracellular Ca^{2+} concentration; CFTR, cystic fibrosis transmembrane conductance regulator; ChTX, charybdotoxin; CLT, clotrimazole; DIDS, 4,4′-diisothiocyanato-stilbene-2,2′-disulphonic acid; DMSO, dimethylsulphoxide; IBMX, isobutylmethylxanthine; I_{SC}, short circuit current; KvLQT1 (KCNQ1), voltage-dependent delayed activated K^+ channel; NPPB, 5-nitro-2-(3-phenylpropylamino)-benzoic acid; PGE_2, prostaglandin E_2; SITS, 4-acetamido-4′-isothiocyanato-stilbene-2,2′-disulphonic acid; SK4, small-conductance Ca^{2+}-activated K^+ channel

Introduction

Chloride (Cl^-) secretion across intestinal epithelium plays a key role in regulating water secretion and is closely regulated by hormonal, neural and paracrine mediators. An increased Cl^- secretion is the major mechanism underlying severe diarrhoea that results in excessive water transport from blood to intestinal lumen (Oprins *et al.*, 2000). It is known that increased intracellular cAMP and cGMP levels play primary roles in activation of the cystic fibrosis transmembrane conductance regulator (CFTR) Cl^- channel in the apical (luminal) membrane of enterocytes (Zhang *et al.*, 1999; Greger, 2000; Albano *et al.*, 2005). In addition, Cl^- secretion by CFTR Cl^- channel in the apical membrane of enterocytes requires the coordinated opening of basolateral K^+ channels to maintain a negative electrical driving force for luminal Cl^- secretion (Greger *et al.*, 1997; McNamara

Correspondence: Professor ZB Hu, Institute of Chinese Materia Medica, Shanghai University of Traditional Chinese Medicine, 1200 Cailun Road, Zhangjiang Hi-tech Park, Shanghai 201203, PR China.
E-mail: zhibihu@hotmail.com
Received 20 August 2007; revised 18 October 2007; accepted 23 November 2007; published online 21 January 2008

et al., 1999). Two types of basolateral (serosal) K^+ channels were found to participate in the process of Cl^- secretion via the apical membrane, namely the cAMP-activated, KCNQ1 channel (voltage-dependent delayed activated K^+ channel) and the Ca^{2+}-activated, SK4 channel (small-conductance Ca^{2+}-activated K^+ channel; Bleich *et al*., 1997; Warth, 2003). Inhibition of both the apical CFTR Cl^- channel and the basolateral cAMP-activated K^+ channel have been recognized as major pharmacological targets for treatment of secretory diarrhoea (Field, 2003).

Extracts of *Berberis aristata* and *Coptis chinensi* have been used in traditional Oriental medicine for the treatment of gastroenteritis and diarrhoea, and it has been suggested that protoberberine alkaloids are the biologically active constituents of these plants (Grycová *et al*., 2007). Berberine is the major medically important, component of the protoberberine alkaloids and this alkaloid prevents epithelial electrolyte secretion in rabbit and rat intestine (Tai *et al*., 1981; Taylor and Baird, 1995) and was an effective treatment for secretory diarrhoea in several small-scale clinical trials (Taylor *et al*., 1999). Block of basolateral K^+ channels was reported to be the mechanism of the antisecretory mechanisms of berberine (Taylor *et al*., 1999). However, it is not known if other protoberberine alkaloids possessed similar effects on ion transport processes during Cl^- secretion. Therefore, in the current study, we selected an allied protoberberine alkaloid, palmatine, and assessed its effect on active ion transport across rat colonic epithelium and elucidated the possible mechanisms underlying its actions. Our results demonstrated that palmatine inhibits chloride secretion in isolated rat distal colon by interfering with both Ca^{2+}- and cAMP-activated pathways of ion transport but through different mechanisms. Thus, palmatine attenuated Ca^{2+}-induced Cl^- secretion by blocking the basolateral charybdotoxin (ChTX)-sensitive SK4 K^+ channel but attenuated cAMP-induced Cl^- secretion by inhibiting the apical CFTR Cl^- channel and the basolateral 293B-sensitive KCNQ1 K^+ channel.

Materials and methods

Animals and tissue preparation

All animal procedures were approved by the University Ethics Committee. Male Wistar rats weighing 200–220 g were obtained from SIPPR/PK Co. Ltd (Shanghai, China). The animals were maintained on a 12–12 h light/dark cycle and allowed free access to normal food and water until the day of experiment. Animals were killed rapidly by stunning and cervical dislocation. A 5-cm segment of the distal colon was removed without distention and placed in ice-cold and oxygen-saturated Parsons solution (Schultheiss *et al*., 2005a) containing (in mM): 107 NaCl, 4.5 KCl, 25 $NaHCO_3$, 1.8 Na_2HPO_4, 0.2 NaH_2PO_4, 1.2 $CaCl_2$, 1.0 $MgSO_4$ and 12 D-glucose (pH 7.4). The colon was opened along the mesenteric border and rinsed free of its faecal contents with Parsons solution. Thereafter, the colon was pinned with the mucosal facing down on a silicon-covered dissection plate, and then, the longitudinal and circular muscles were carefully stripped away with fine forceps. Finally, the isolated mucosal sheet was cut into an appropriate size for the Ussing chamber.

Measurement of electrophysiological parameters

Freshly isolated rat colonic mucosal sheets were fixed to holding sliders and mounted in modified Ussing chambers (EasyMount Chamber; Physiologic Instruments, San Diego, CA, USA) with a window area of 0.5 cm^2. Two pieces of mucosal sheet were used from each animal. Tissues were bathed on both mucosal and serosal sides with 5 ml of Parsons solution that was maintained at 37 °C by heated water jackets and the pH was maintained at 7.4 by oxygenation with a gas mixture (95% O_2/5% CO_2). The tissues were voltage clamped at 0 mV to monitor short circuit current (I_{SC}) using a Dual Voltage Clamp amplifier (VCC MC2; Physiologic Instruments) connected via an ADI Instruments PowerLab 8SP to a computer. The transepithelial electrical potential (PD) was measured by a pair of pipette-shaped voltage-sensing electrodes made of sintered Ag–AgCl wire (Physiologic Instruments) in agar bridges filled with a solution of 4% (w/v) agarose in 3 M KCl solution; the electrical current across mucosae was measured by a pair of pipette-shaped current-passing electrodes made of Ag pellet (Physiologic Instruments) in agar bridges filled with a solution of 4% (w/v) agarose in 3 M KCl solution. The current deflection (ΔI_{SC}) was caused by applying a 1-mV pulse for 0.5 at 60 s intervals under short circuit condition through the voltage-sensing electrodes. By this procedure, the transepithelial electrical resistance (R_{te}) can be calculated by Ohm's law ($R_{te} = PD/\Delta I_{SC}$). A positive I_{SC} is referred as a net flow of anions from the basolateral to the apical side, a net flow of cations from the apical to the basolateral side or a combination of each.

Measurement of apical membrane Cl^- current and basolateral membrane K^+ current

The apical membrane Cl^- current (I_{Cl}) was investigated according to Schultheiss *et al*. (2005a). Briefly, the basolateral membrane was depolarized with a solution containing high potassium concentrations, for more than 40 min. Then, apical Cl^- current was measured in the presence of a serosal-to-mucosal Cl^- gradient with the following bath solution: apical (in mM), 107 K-gluconate, 4.5 KCl, 25 $NaHCO_3$, 1.8 Na_2HPO_4, 0.2 NaH_2PO_4, 5.75 Ca-gluconate, 1.0 $MgSO_4$ and 12 glucose; basolateral (in mM), 111.5 KCl, 25 $NaHCO_3$, 1.8 Na_2HPO_4, 0.2 NaH_2PO_4, 1.25 $CaCl_2$, 1.0 $MgSO_4$ and 12 D-glucose. This procedure allows measurement of changes in the apical anion conductance, avoiding contamination in the current response from, for instance, ChTX-sensitive apical K^+ channel (Schultheiss *et al*., 2005a).

The basolateral membrane K^+ current (I_K) was determined after permeabilization of the apical membrane with nystatin (100 $\mu g\,ml^{-1}$ on the mucosal side) in the presence of a mucosal-to-serosal K^+ gradient (13.5 mM KCl at the mucosal side and 4.5 mM KCl at the serosal side) (Schultheiss *et al*., 2005a) established by the following bath solution: apical (in mM), 98 *N*-methyl-D-glucamine (NMDG)-Cl, 13.5 KCl, 25 choline HCO_3^-, 1.8 Na_2HPO_4, 0.2 NaH_2PO_4, 1.25 $CaCl_2$, 1.0 $MgSO_4$ and 12 D-glucose; basolateral (in mM), 107 K-gluconate, 4.5 KCl, 25 $NaHCO_3$, 1.8 Na_2HPO_4, 0.2 NaH_2PO_4, 5.75 Ca-gluconate, 1.0 $MgSO_4$ and 12 D-glucose. All solutions were adjusted to pH 7.4 at 37 °C.

Measurement of intracellular Ca^{2+} concentration

Crypts were isolated from rat distal colon as previously described (Leipziger *et al*., 1997). Briefly, the distal colon was resected and turned inside out. The inverted sac was filled with 5 ml of the Ca^{2+}-free EDTA solution (in mM): 127 NaCl, 5 KCl, 5 Na-pyruvate, 1.0 $MgCl_2$, 5 EDTA, 5 D-glucose, 10 HEPES, with 1 g l^{-1} BSA. The solution was oxygenated with 100% O_2 and pH was adjusted to 7.4 by Tris-base. The sac was incubated in the above-mentioned solution for 10 min at 37 °C. The isolated crypts were collected by shaking the sacs and kept in a Ringer solution with the following composition (in mM): 127 NaCl, 5 KCl, 5 Na-pyruvate, 1.0 $MgCl_2$, 1.2 $CaCl_2$, 5 D-glucose, 10 HEPES, with 1 g l^{-1} BSA; pH of 7.4. For measurement of intracellular Ca^{2+} concentration ($[Ca^{2+}]_i$), the isolated crypts were loaded with 3 μM Fura-2-acetoxymethylester (Fura-2 AM) in Ringer solution containing pluronic F127 (0.025%) at 25 °C for 60 min. The Fura-2-loaded crypts were washed with the Ringer solution and attached to the glass coverslip precoated with poly (L-lysine). The coverslip was then attached to the bottom of a 250-μl perspex perfusion chamber mounted on the stage of an inverted microscope (IX-70; Olympus Optical Co., Tokyo, Japan) and crypts were continuously superfused with the Ringer solution at a rate of 2 ml min^{-1} at room temperature. Fluorescence images were acquired with a digital CCD camera (C4742-95-12NRB; Hamamatsu Photonics KK, Hamamatsu, Japan). A high-speed scanning polychromatic light source (C7773, Hamamatsu Photonics) was used for alternate excitations at wavelengths of 340 and 380 nm. The fluorescence images at both wavelengths (F340 and F380) were measured using PC-based software (Aquacosmos Ver1.2, Hamamatsu Photonics) every 5 s. Autofluorescence in F340 and F380 was examined in the colonic crypts without dye loading, and the values were subtracted from the data acquired after dye loading. The image ratio of F340 to F380 (F340/F380) was calculated from the subtracted data.

Measurement of intracellular cAMP content

Cytosolic cAMP content was measured with an enzyme immunoassay. The isolated mucosal sheets were equilibrated in Ussing chambers with the normal Parsons solution at 37 °C for 90 min and then the tissues were further preincubated with or without palmatine (serosal) for 30 min. After this preincubation, the tissues were exposed to 100 μM isobutylmethylxanthine (IBMX) or 100 μM IBMX plus 5 μM forskolin for 15 min at both sides, and then rapidly frozen in liquid nitrogen and stored at −80 °C until homogenized in 0.5 ml of ice-cold 6% trichloracetic acid using a glass homogenizer. The homogenate was centrifuged at 2000 *g* for 10 min at 4 °C. The supernatant was extracted three times with three volumes of diethyl ether before lyophilization. cAMP level was assayed by a cAMP enzyme immunoassay kits (Cayman Chemical Co., Ann Arbor, MI, USA; R&D Systems, Minneapolis, MN, USA). The tissue residue was dissolved in 2 M NaOH, and protein content was determined using a protein assay kit (Sigma, St Louis, MO, USA) with BSA as the standard. The concentration of cAMP was expressed as pmol mg^{-1} protein.

Data analysis

Results are presented as the mean ± s.e.mean. The number of tissue preparations was indicated by *n*. The difference between two different groups was analysed by Student's paired or unpaired *t*-test. The differences among multiple groups were analysed by one-way ANOVA. Probability (*P*) value of less than 0.05 was considered to indicate statistical significance. The changes in I_{SC} (ΔI_{SC}) were quantified by subtracting its respective baseline values before drug administration, from the peak of a current response. The IC_{50} value was calculated from nonlinear regression analysis of dose–response data by GraphPad Prism software version 4.03 (GraphPad Prism software Inc., San Diego, CA, USA).

Chemicals

Chemically pure palmatine was obtained from Laboratory of Chemistry, Institute of Chinese Materia Medica, Shanghai University of Traditional Chinese Medicine; it was identified on the basis of chemical and spectroscopic evidence. Atropine, bumetanide, carbachol, ChTX, clotrimazole (CLT), 8-bromoadenosine 3′,5′-cyclic monophosphate (8-bromo-cAMP), 4,4′-diisothiocyanato-stilbene-2,2′-disulphonic acid (DIDS), forskolin, IBMX, ionomycin, nystatin, prostaglandin E_2 (PGE_2) and 4-acetamido-4′-isothiocyanato-stilbene-2,2′-disulphonic acid (SITS) were obtained from Sigma-Aldrich. Chromanol 293B (293B) was purchased from Tocris (Ellisville, MO, USA), glibenclamide was from BIOMOL (Biomol Research Labs. Inc., Plymouth Meeting, PA, USA), and 5-nitro-2-(3-phenylpropylamino)-benzoic acid (NPPB) was obtained from Calbiochem (La Jolla, CA, USA). Fura-2-acetoxymethylester (Fura-2 AM) and pluronic F127 were purchased from Dojindo Laboratories (Kumamoto, Japan). CFTR inhibitor 172 was a kind gift from Dr TH Ma (Membrane Channel Research Laboratory, Northeast Normal University, Changchun, Jilin Province, PR China).

Palmatine hydrochloride, carbachol, ChTX and 8-bromo-cAMP were dissolved to give aqueous stock solutions and diluted in buffer just before use. All other drugs were dissolved in dimethylsulphoxide and final dimethylsulphoxide concentration was less than 0.1% (v/v). For permeabilization studies, nystatin was used as 100 mg ml^{-1} stock solution in dimethylsulphoxide (final concentration 0.1% v/v) and sonicated for 30 s just before use. If drugs were dissolved in a solvent other than aqueous solution, the same volume of solvent was administered to the control tissue.

Results

Effect of palmatine on Ca^{2+}- and cAMP-activated chloride secretion in rat distal colon

Following a 90-min equilibration with normal Parsons solution, the average transepithelial potential (PD), I_{SC} and transepithelial resistance (R_{te}) were -3.97 ± 0.1 mV, 36.4 ± 0.8 μA cm^{-2} and 110.8 ± 1.4 Ω cm^2 in rat colon preparations ($n = 529$), respectively. Application of 100 and 300 μM palmatine to both sides did not influence the basal I_{SC} or R_{te}.

Application of the muscarinic acetylcholine receptor agonist, carbachol (50 μM), to basolateral side evoked a biphasic increase in I_{SC} including fast (transient) and slow

(sustained) phases. The transient phase was observed at 2–3 min and the sustained phase at 10 min after the addition of carbachol. Carbachol-evoked transient and sustained values were 231.6 ± 10.3 and $96.7 \pm 5.6\,\mu A\,cm^{-2}$ ($n=23$), respectively. Carbachol-induced I_{SC} was not inhibited by pretreatment of tissues with an epithelial Na^+ channel inhibitor amiloride (100 μM, apical), suggesting that carbachol-induced increase in I_{SC} was mainly carried by Cl^- ion. When the tissues were preincubated with various concentrations of palmatine (1–300 μM, on the serosal but not mucosal side) for 30 min, the carbachol-induced transient and sustained responses were diminished in a concentration-dependent manner (Figure 1a). Analysis of the concentration–response curves revealed that palmatine maximally inhibited the carbachol-induced transient and sustained increases in I_{SC} by $84.9 \pm 2.2\%$ with an IC_{50} of 24.0 ± 4.7 μM and $80.7 \pm 3.2\%$ with an IC_{50} of 29.2 ± 6.1 μM, respectively (Figures 1b and c). The inhibitory effect of palmatine on the carbachol-induced I_{SC} was reversible. Addition of 50 μM carbachol to the basolateral side of the preparation produced transient and sustained increases in I_{SC} of 218.8 ± 13.5 and $81.0 \pm 4.7\,\mu A\,cm^{-2}$, respectively ($n=8$). These responses were reduced to $47.5 \pm 4.6\,\mu A\,cm^{-2}$ (transient) and $10.3 \pm 3.1\,\mu A\,cm^{-2}$ (sustained) by pretreatment of tissue with 100 μM palmatine for 30 min. Following washout of the palmatine, the carbachol-induced I_{SC} returned to $158.8 \pm 8.9\,\mu A\,cm^{-2}$ (transient) and $69.8 \pm 3.2\,\mu A\,cm^{-2}$ (sustained). Because application of 100 μM palmatine to the serosal side caused a maximal inhibition in the I_{SC} response to carbachol, this concentration was used to compare the responses between control and treated samples in the subsequent experiments on Ca^{2+}-activated responses.

Carbachol-stimulated Cl^- secretion was mimicked by a Ca^{2+} ionophore, ionomycin. After ionomycin application, a Ca^{2+}-activated I_{SC} was developed, presenting a transient peak followed by a plateau phase. Both the phases were diminished by pretreating the tissue (basolateral but not apical side) with 100 μM palmatine for 30 min (Figure 2).

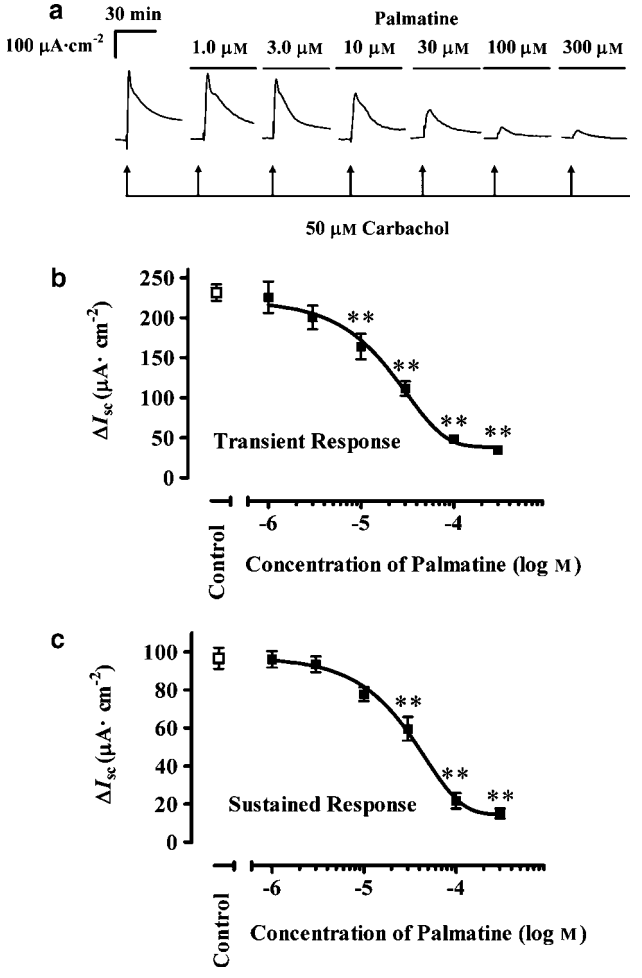

Figure 1 Inhibitory effect of palmatine on the carbachol-evoked short circuit current (I_{SC}) in isolated rat colonic mucosa. (**a**) Inhibition of carbachol-evoked I_{SC} in rat colonic mucosa by preincubation with various concentrations of palmatine (1.0–300 μM, serosal). Examples of original recordings are shown. Each concentration of palmatine was added as a single dose to separate tissues for 30 min before addition of carbachol (50 μM, serosal). (**b** and **c**) Summary of the concentration-dependent inhibitory effect of palmatine on carbachol-evoked I_{SC}, data collected from experiments as shown in (**a**). Data are expressed as net decrease compared with carbachol-evoked I_{SC} (ΔI_{SC}) during transient (**b**) and sustained (**c**) phases. Each point represents mean ± s.e.mean ($n=8$–23), significantly different from the carbachol-evoked I_{SC} with $^*P<0.05$ and $^{**}P<0.01$.

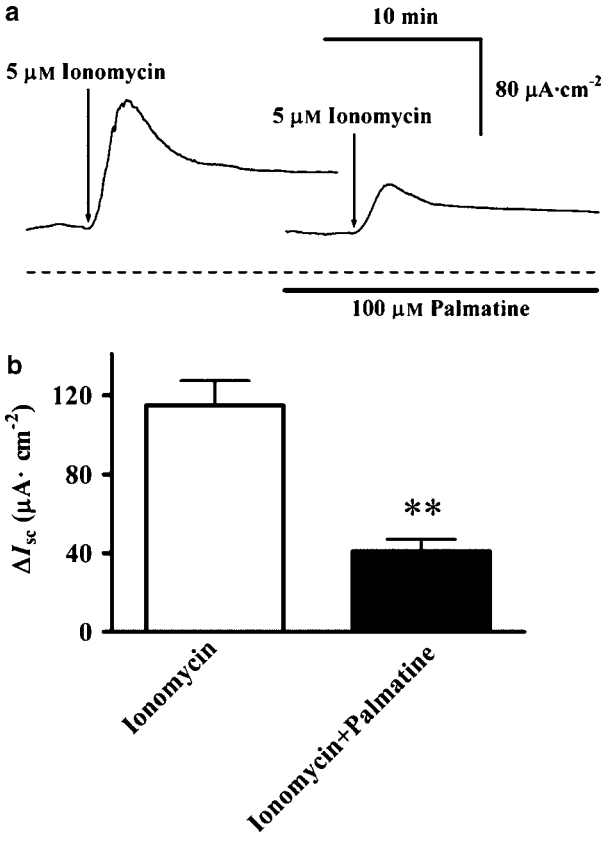

Figure 2 Inhibitory effect of palmatine on the ionomycin-evoked short circuit current (I_{SC}) in isolated rat colonic mucosa. (**a**) The inhibition in ionomycin-evoked I_{SC} in rat colonic mucosa by preincubation with palmatine (100 μM, serosal). Examples of original recordings are shown. Palmatine was added for 30 min before addition of ionomycin (5 μM, serosal). Dashed line indicates zero current level. (**b**) Summary data showing mean ΔI_{SC} in response to ionomycin in the presence and absence of palmatine. Data are mean ± s.e.mean ($n=10$). $^{**}P<0.01$, significantly different from the value in the absence of palmatine.

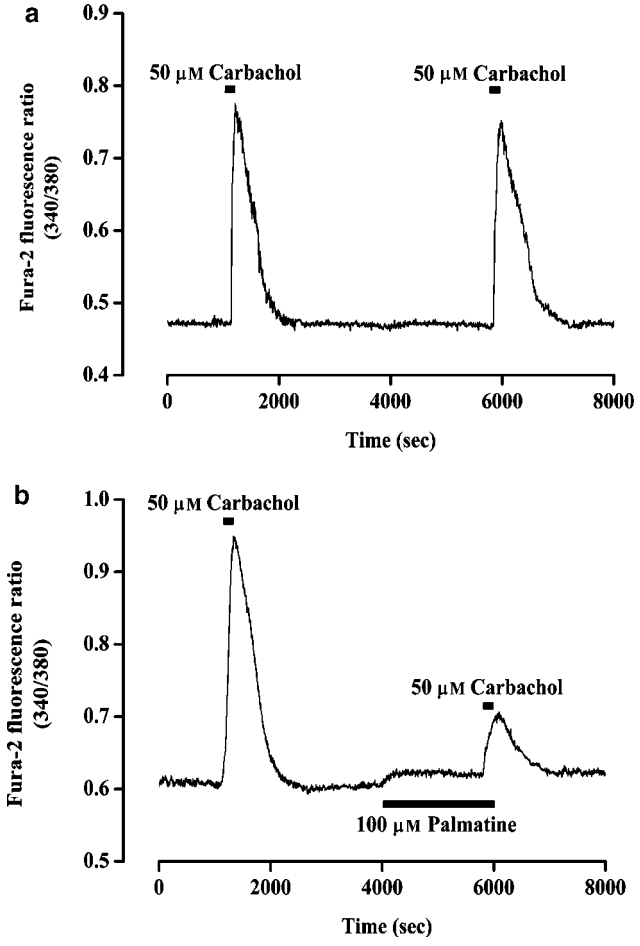

Figure 3 Effect of palmatine on carbachol-induced increase in intracellular Ca^{2+} concentration ($[Ca^{2+}]_i$) in colonic crypts. (**a**) Effect of repeated application of carbachol (50 μM) on increases in $[Ca^{2+}]_i$. (**b**) The rise in $[Ca^{2+}]_i$ induced by carbachol (50 μM) was inhibited by pretreatment of crypts with palmatine (100 μM) for 30 min.

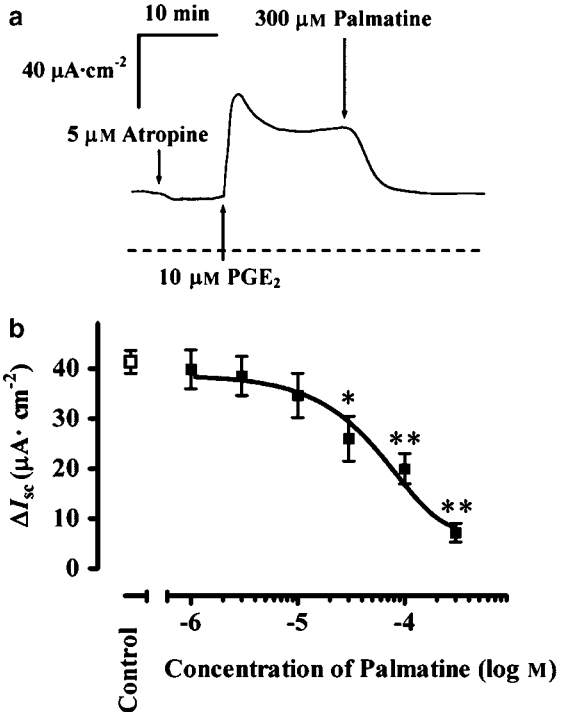

Figure 4 Inhibitory effect of palmatine on the prostaglandin E_2 (PGE_2)-evoked short circuit current (I_{SC}) in isolated rat colonic mucosa. (**a**) An original recording showing effect of palmatine (300 μM, serosal) on I_{SC} in the plateau phase observed after addition of PGE_2 (10 μM, serosal) in the presence of atropine (5 μM, serosal). Dashed line indicates zero current level. (**b**) Summary of the concentration-dependent inhibitory effect of palmatine on PGE_2-evoked I_{SC}, data collected from experiments as shown in (**a**). Each concentration of palmatine was added as a single treatment to separate tissues when the plateau phase was observed after addition of PGE_2 (10 μM, serosal) in the presence of atropine (5 μM, serosal). Values are expressed as net decrease compared with PGE_2-evoked I_{SC} (ΔI_{SC}). Besides control ($n=46$), each point represents mean ± s.e.mean ($n=4$–5). *$P<0.05$ and **$P<0.01$, significantly different from PGE_2-evoked I_{SC}.

We subsequently investigated whether palmatine interfered with the increase in $[Ca^{2+}]_i$ evoked by carbachol in Fura-2-loaded crypts. Superfusion of crypts with 50 μM carbachol caused an increase of the Fura-2 fluorescence ratio (Figure 3a) from a value of 0.61 ± 0.02 to 0.97 ± 0.02 within 3 min ($P<0.01$; $n=18$) (Figure 3b). Pretreatment of crypts with 100 μM palmatine for 30 min and carbachol (50 μM) only induced a very small increase of the ratio from a value of 0.62 ± 0.02 to 0.69 ± 0.02 ($P<0.01$ versus response in the absence of palmatine; $n=18$) (Figure 3b). These data demonstrated that palmatine inhibited the carbachol-activated Cl^- secretion by preventing the rise in $[Ca^{2+}]_i$ evoked by carbachol.

The effects of palmatine on Cl^- secretion were also examined by using another stimulus for Cl^- secretion, raised intracellular cAMP concentration. This was achieved with PGE_2, forskolin or 8-bromo-cAMP.

In colonic epithelia, PGE_2 increases intracellular cAMP level via the EP_2 receptor and activates both the apical CFTR and basolateral cAMP-dependent K^+ channels (McNamara *et al*., 1999). PGE_2, also acts on the submucosal plexus, stimulating Cl^- secretion in the isolated rat colonic mucosa (Suzuki *et al*., 2000). In the present study, the indirect stimulatory action of PGE_2 via the submucosal plexus was inhibited by atropine and the direct action of PGE_2 on the mucosa was measured (Figure 4a). In the presence of atropine (5 μM, serosal), the addition of PGE_2 (10 μM, serosal) induced an increase in I_{SC} of 41.3 ± 2.2 μA cm^{-2} ($n=46$). The serosal addition of palmatine inhibited this PGE_2-induced increase in I_{SC} in a concentration-dependent manner with an IC_{50} value of 61.9 ± 22.0 μM (Figure 4b).

Forskolin, an adenylate cyclase activator, stimulates Cl^- secretion by increasing intracellular cAMP contents in many tissues and cells (Gabriel *et al*., 1999; Leung *et al*., 2001; Resta-Lenert *et al*., 2001). Addition of forskolin (5 μM) to both sides induced a rise in I_{SC} that reached to a peak value after 10 min, and was then maintained at sustained level after 20 min. Administration of palmatine to the basolateral bath during the sustained phase caused a concentration-dependent reduction of the forskolin response (Figure 5a). Analysis of the concentration–response curves revealed that the maximal inhibitory response of I_{SC} to palmatine was 53.9 ± 3.1% and half this maximal response was attained at 68.7 ± 19.6 μM (Figure 5b). The inhibitory effect of palmatine on the forskolin-induced I_{SC} was reversible. Application of

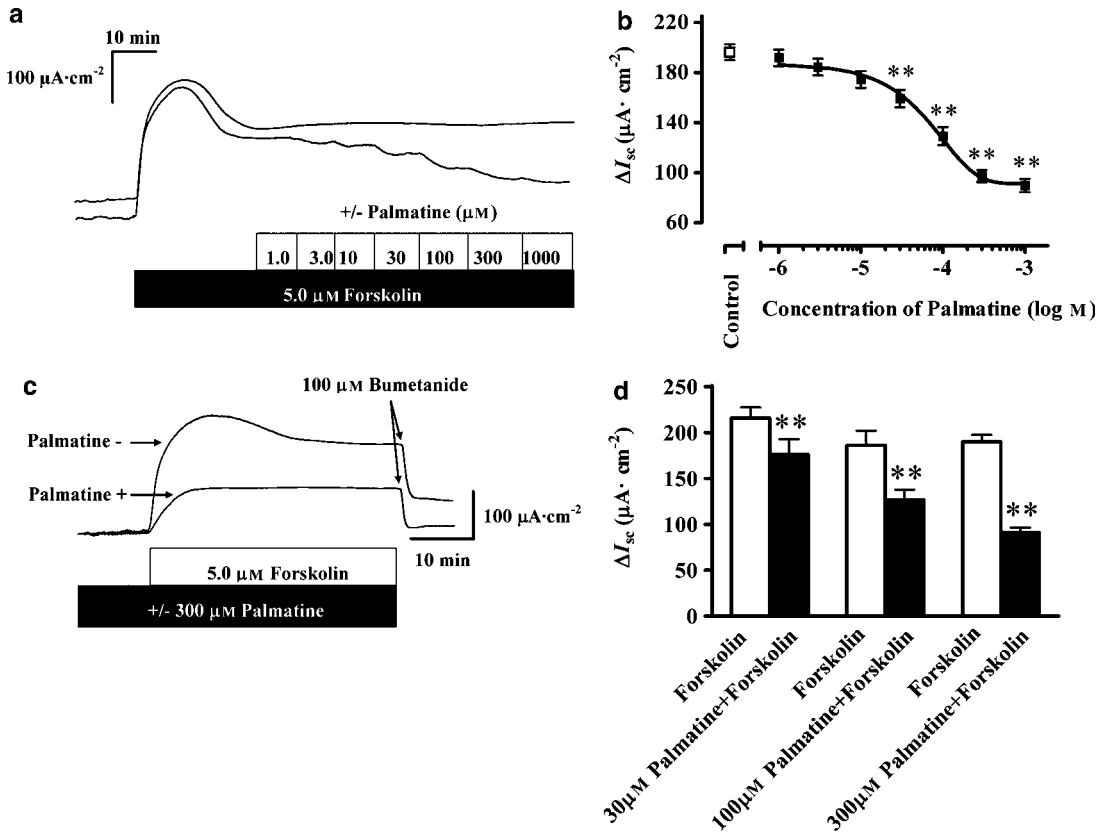

Figure 5 Inhibitory effect of palmatine on the forskolin-evoked short circuit current (I_{SC}) in isolated rat colonic mucosa. (**a**) Original recordings showing the concentration-dependent inhibition of I_{SC} by palmatine in the presence of forskolin (5 μM, bilateral). Palmatine (1.0–1000 μM, serosal) was added cumulatively, as indicated after the forskolin-elicited response reached the plateau phase. (**b**) Summary of the concentration-dependent inhibitory effect of palmatine on the forskolin-evoked I_{SC}, data collected from experiments as shown in (**a**). Values are expressed as net inhibition of the forskolin-evoked I_{SC} before the addition of palmatine (ΔI_{SC}). Each point represents mean ± s.e.mean ($n=8$). *$P<0.05$ and **$P<0.01$, significantly different from forskolin-evoked I_{SC}. (**c**) Original recordings showing the forskolin-evoked I_{SC} in the presence and absence of palmatine. Forskolin (5 μM, bilateral) was added as indicated. Palmatine (300 μM, serosal) was added 30 min before addition of forskolin (5 μM, bilateral). Bumetanide (100 μM, serosal) strongly inhibited the forskolin-elicited response at its plateau phase in the presence or absence of palmatine. (**d**) Summary data showing mean ΔI_{SC} in response to forskolin in the presence and absence of palmatine collected from experiments as shown in (**c**). Each column represents mean ± s.e.mean ($n=6$). **$P<0.01$, significantly different from the corresponding values without palmatine.

5 μM forskolin to the both sides produced an increase in I_{SC} of $183.3 \pm 10.1\ \mu A\ cm^{-2}$ ($n=6$). After pretreatment of tissue with 300 μM palmatine for 30 min, the forskolin-induced I_{SC} was reduced to $84.6 \pm 3.0\ \mu A\ cm^{-2}$. On washout of palmatine, the forskolin-induced I_{SC} returned to $173.3 \pm 15.4\ \mu A\ cm^{-2}$. Because application of 300 μM palmatine to the serosal side caused a maximal inhibition in the I_{SC} response to forskolin, this concentration was used to compare the responses between control and treated samples in the subsequent experiments on cAMP-activated responses.

The forskolin-stimulated I_{SC} was inhibited by bumetanide, an inhibitor of the Na^+-K^+-$2Cl^-$ cotransporter, in the presence and absence of palmatine (Figure 5c), confirming that the forskolin-stimulated I_{SC} was due to Cl^- secretion. Inhibition of forskolin-evoked Cl^- secretion by palmatine was only effective when palmatine was added to the basolateral side of the preparation and not to the apical side (Figures 5c and d).

The effect of palmatine on cAMP-induced Cl^- secretion, without activation of the adenylate cyclase, was evaluated with the membrane permeable cyclic AMP analogue, 8-bromo-cAMP. The addition of 8-bromo-cAMP (100 μM, bilaterally) induced a sustained increase in I_{SC}, which was inhibited by addition of palmatine (300 μM) to the serosal side (Figure 6).

Effect of palmatine on apical chloride current

Because palmatine prevented both Ca^{2+}- and cAMP-mediated Cl^- secretion, further experiments were carried out to identify the apical Cl^- channels involved. The Cl^- currents across the apical membrane were measured after depolarization of the basolateral membrane with high K^+ solution in the presence of a basolateral-to-apical Cl^- gradient. Figure 7a shows that application of carbachol induced a transient increase in an outward current, which, under these conditions, represented an increased Cl^- efflux across the apical membrane and showed activation of a Ca^{2+}-dependent transient Cl^- current. This current was not affected by pretreatment with palmatine (control I_{Cl}, $20.1 \pm 2.2\ \mu A\ cm^{-2}$, $n=7$; pretreatment with palmatine, $17.7 \pm 1.6\ \mu A\ cm^{-2}$, $n=7$), but was significantly inhibited

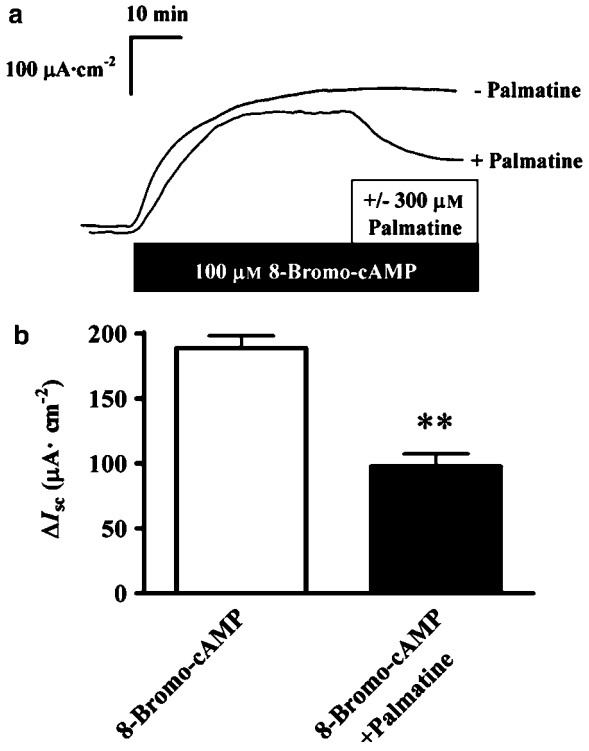

Figure 6 Inhibitory effect of palmatine on 8-bromo-cAMP-evoked short circuit current (I_{SC}) in isolated rat colonic mucosa. (**a**) Original recordings showing 8-bromo-cAMP-evoked I_{SC} before and after addition of palmatine. 8-bromo-cAMP (100 μM, bilateral) was added as indicated. Palmatine (300 μM, serosal) was added 30 min after addition of 8-bromo-cAMP (100 μM, bilateral). (**b**) Summary data showing mean ΔI_{SC} in response to 8-bromo-cAMP before and after addition of palmatine. Each column represents mean ± s.e.mean ($n=6$). **$P<0.01$, significantly different from the corresponding values in the absence of palmatine.

by pretreatment with SITS (100 μM) (control I_{Cl}, $18.7 \pm 1.7\,\mu A\,cm^{-2}$, $n=6$; pretreatment with SITS, $8.7 \pm 1.4\,\mu A\,cm^{-2}$, $n=6$; $P<0.01$) (Figures 7a and b). These results indicated that the inhibition of carbachol-induced Cl^- secretion by palmatine did not involve a direct inhibition of the apical Ca^{2+}-activated Cl^- channels.

We then tested the involvement of apical Cl^- channels in the cAMP-activated Cl^- secretion under the same conditions. Addition of forskolin (5 μM, bilateral) resulted in an increase in an outward current by $65.4 \pm 2.1\,\mu A\,cm^{-2}$ ($n=31$), illustrated in Figure 7c. Then a range of different Cl^- channel inhibitors, such as CFTR inhibitor 172, glibenclamide, NPPB and DIDS, and palmatine were added prior to activation of I_{Cl} by forskolin. As illustrated in Figure 7d, this current was not affected by pretreatment with DIDS (500 μM, mucosal) but was significantly inhibited by pretreatment with palmatine (300 μM, serosal, $n=8$; $P<0.01$), CFTR inhibitor 172 (20 μM, mucosal; $n=6$; $P<0.01$), glibenclamide (500 μM, mucosal; $n=6$; $P<0.01$) or NPPB (100 μM, mucosal; $n=6$; $P<0.01$).

Effect of palmatine on basolateral K^+ currents

To determine the direct effect of palmatine on the basolateral K^+ currents, the K^+ currents across the basolateral membrane were measured after permeabilization of the apical membrane with nystatin in the presence of an apical-to-basolateral K^+ gradient with K^+ as the sole permeant ion. In the presence of a K^+ gradient, nystatin (100 μM; mucosal) evoked a basal I_K in rat colon mucosal sheets (Figures 8a and b). This current was unaffected by pretreatment with palmatine (300 μM, serosal; $n=6$), ChTX (100 nM, serosal; $n=6$), 293B (30 μM, serosal; $n=6$) or CLT, a dual blocker of Ca^{2+}- and cAMP-dependent K^+ channels (30 μM, serosal; $n=5$) (Figure 8b). Subsequently, when nystatin-evoked basal I_K had reached a semi-steady-state condition, addition of carbachol (50 μM) to the basolateral membrane stimulated a further increase in outward current corresponding to activation of basolateral Ca^{2+}-dependent K^+ channels (Figures 8a and b). This current was inhibited by pretreatment with palmatine (100 μM, serosal; $n=6$; $P<0.01$), ChTX (100 nM, serosal; $n=6$; $P<0.01$) and CLT (30 μM, bilateral; $n=5$; $P<0.01$), but was insensitive to pretreatment with 293B (30 μM, serosal; $n=6$) (Figure 8c).

Under the same conditions, involvement of the cAMP-activated K^+-channels was assessed. After nystatin-evoked basal I_K had reached the semi-steady-state condition, addition of forskolin (5 μM, bilateral) further evoked an outward current, consistent with activation of basolateral cAMP-dependent K^+ channels (Figures 9a and b). This current was inhibited by pretreatment with palmatine (300 μM, serosal; $n=6$; $P<0.01$), 293B (30 μM, serosal;, $n=6$; $P<0.01$) and CLT (30 μM, bilateral; $n=6$; $P<0.01$), but was insensitive to pretreatment with ChTX (100 nM, serosal; $n=6$) (Figure 9c).

Effect of palmatine on the intracellular cAMP content

To explore whether the inhibition of Cl^- secretion induced by forskolin involved the alteration of intracellular cAMP content, the intracellular cAMP content of rat colon mucosa determined with an enzyme immunoassay. Under control condition, the intracellular cAMP content was low (Figure 10; $n=9$) and stimulating preparations with 5 μM forskolin led to a significant elevation (about 10-fold) in the cytosolic cAMP concentration ($n=8$). Pretreatment with palmatine at concentration of 300 μM did not influence the basal cAMP level ($n=9$) compared with control value, but significantly inhibited forskolin-induced elevation of cAMP levels in a concentration-dependent manner (Figure 10).

Discussion

Protoberberine alkaloids are components of *Berberis*, *Mahonia* and *Coptis* with a long history of use as folk medicine (Racková *et al*., 2004). Berberine and palmatine are the most medically significant members of the protoberberine alkaloids. They have the same tetracyclic structure but differ in the nature of the subsitituents on the benzo ring, this being methylene dioxy for berberine and dimethoxy for palmatine (Giri *et al*., 2006). Protoberberine alkaloids exhibit a wide variety of pharmacological and biological activities including antisecretory, anti-inflammatory, antimicrobial, antimalarial and anticancer actions (Shin *et al*., 2000; Da-Cunha *et al*., 2005). In addition, protoberberine alkaloids are highly

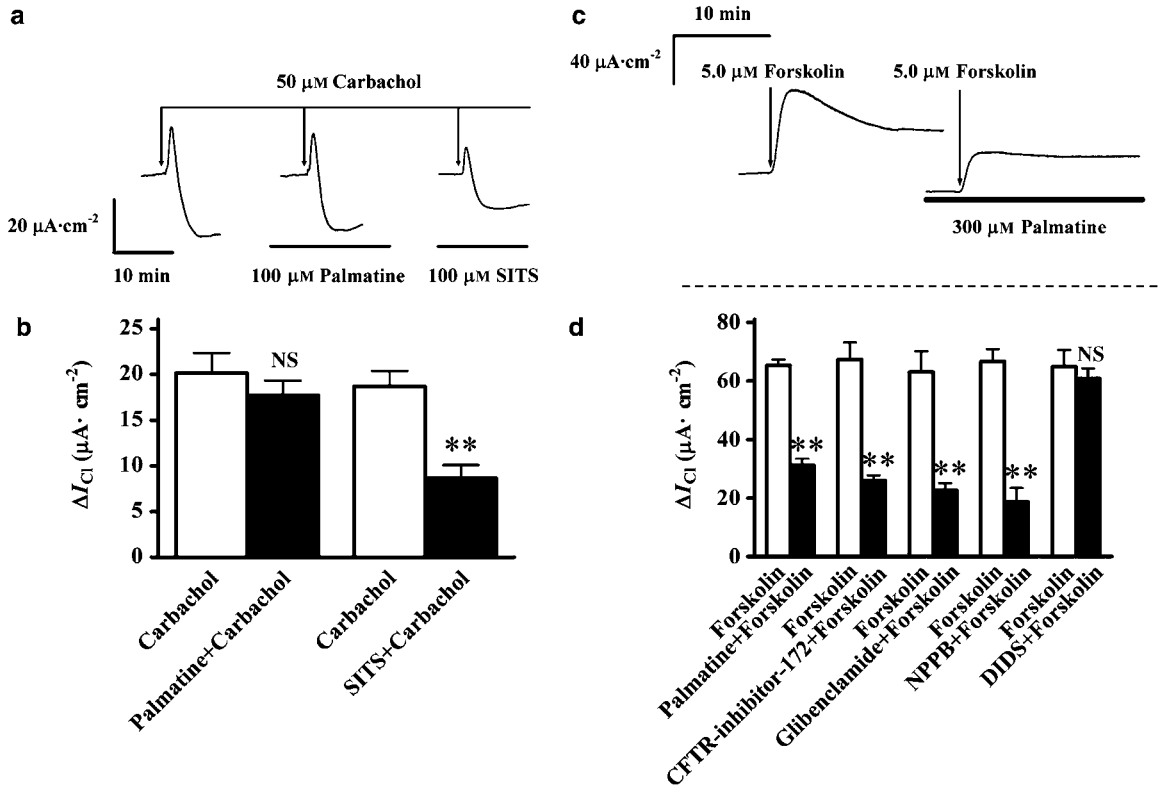

Figure 7 Effect of palmatine on Cl^- current (I_{Cl}) across the apical membrane in isolated rat colonic mucosa. (**a**) After establishment of a basolateral-to-apical Cl^- gradient in the high K^+ solution by depolarization of the basolateral membrane, addition of carbachol (50 μM, serosal) evoked an outward current, consistent with a flux of Cl^- from the basolateral to apical side. This current was inhibited by pretreatment with SITS (100 μM, mucosal) but not with palmatine (100 μM, serosal). (**b**) Summary data showing mean ΔI_{Cl} in response to carbachol in the presence or absence of palmatine (100 μM, serosal) and SITS (100 μM, mucosal). Each column represents mean ± s.e.mean ($n = 6$–7). $^{**}P < 0.01$, significantly different from the corresponding carbachol-evoked I_{Cl}. NS, not sufficiently different from the control. (**c**) After establishment of a basolateral-to-apical Cl^- gradient by depolarization of the basolateral membrane with high K^+ solution, addition of forskolin (5 μM, bilateral) elicited an outward current, consistent with a secretory Cl^- flow. This current was inhibited by pretreated with palmatine (300 μM, serosal). Dashed line indicates zero current level. (**d**) Summary data showing mean ΔI_{Cl} in response to forskolin in the presence of palmatine (300 μM, serosal), cystic fibrosis transmembrane conductance regulator (CFTR) inhibitor 172 (20 μM, mucosal), NPPB (100 μM, mucosal), DIDS (500 μM, mucosal) and glibenclamide (500 μM, mucosal). Each column represents mean ± s.e.mean ($n = 5$–6). $^{**}P < 0.01$, significantly different from the corresponding forskolin-evoked I_{Cl}. NS, not sufficiently different from the control.

effective as cytotoxic and antileukaemic agents against human fibroblast and premyelocytic leukaemic cells (Subeki *et al.*, 2005). Although the antisecretory mechanism of berberine has been reported, nothing is known about the role of other protoberberine alkaloids such as palmatine on ion transport, particularly Cl^- secretion. Our study has shown that palmatine markedly inhibited Cl^- secretion in isolated distal colon through its actions on both Ca^{2+}- and cAMP-activated pathways for ion transport. Apart from these two different activation pathways, Cl^- secretion in polarized epithelia requires parallel activation of two different types of ion channel, luminal Cl^- channels and basolateral K^+ channels, to generate the driving force for Cl^- exit into the lumen. Our results showed that both types of ion channels were inhibited by palmatine.

Ca^{2+}- and carbachol-activated Cl^- secretion

In respiratory epithelium and T84 cells, Ca^{2+}-activated Cl^- secretion is mediated by the apical Ca^{2+}-dependent Cl^- channel (Kunzelmann and Mall, 2002). However, there is no clear evidence that Ca^{2+} directly activates the apical Cl^- channel in the colonic crypt cells of the native tissue (Strabel and Diener, 1995; Mall *et al.*, 1998). In contrast, a carbachol-activated transient Ca^{2+}-dependent Cl^- current at the apical membrane has been recently reported by Schultheiss *et al.* (2005b). This current was sensitive to SITS, a nonspecific blocker of Ca^{2+}-dependent Cl^- channels, and dependent on the presence of mucosal Ca^{2+}. In the present study, depolarizing the basolateral membrane with high K^+ solution in the presence of a basolateral-to-apical Cl^- gradient revealed a carbachol-induced Ca^{2+}-dependent Cl^- current in the apical membrane that was inhibited by SITS but not by palmatine, indicating that the apical Ca^{2+}-dependent Cl^- channel was not a target of palmatine action when the Ca^{2+}-mediated Cl^- secretion was inhibited. Inhibition of the carbachol-induced increase of $[Ca^{2+}]_i$ by palmatine is in accordance with the general model of Ca^{2+}-dependent Cl^- secretion, in which carbachol induces an IP_3-mediated increase of the cytoplasmic Ca^{2+} concentration, leading to a hyperpolarization of the membrane and an increase in driving force for Cl^- secretion (Schultheiss *et al.*,

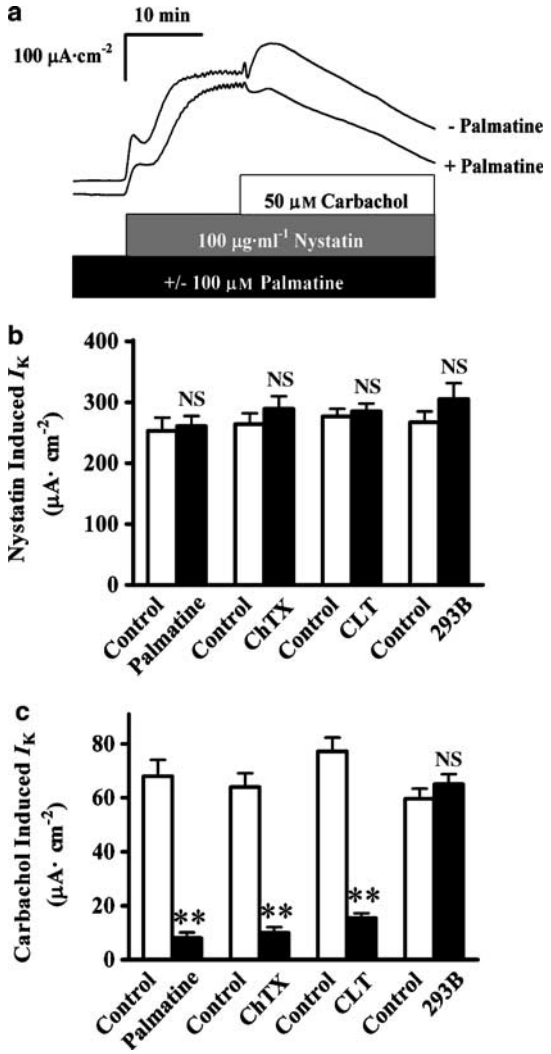

Figure 8 Effect of palmatine on Ca^{2+}-dependent K^+ current (I_K) across basolateral membrane in isolated rat colonic mucosa. The K^+ current across the basolateral membrane was measured after permeabilization of the apical membrane with nystatin (100 μg ml^{-1}, mucosal) in the presence of an apical-to-basolateral K^+ gradient with K^+ as the sole permeant ion. (**a**) Original recordings showing the basal and carbachol-evoked outward I_K pretreated with or without palmatine (100 μM, serosal) in nystatin-permeabilized rat distal colon. (**b**) Effect of palmatine and different K^+ blockers in nystatin-permeabilized rat distal colon. Palmatine (100 μM, serosal), charybdotoxin (ChTX; 100 nM, serosal), chromanol 293B (293B; 30 μM, serosal) and clotrimazole (CLT; 30 μM, bilateral) were preincubated for 30 min. (**c**) Carbachol (50 μM) was added to the serosal bath 30 min after pretreatment with palmatine and blockers in the same experiments as (**b**). Each column shown in (**b**) and (**c**) represents mean ± s.e.mean ($n = 5$–6). $^{**}P < 0.01$, significantly different from the respective controls. NS, not significantly different from the respective controls.

2005b). Such changes in $[Ca^{2+}]_i$ could also affect the basolateral K^+ channels and these were studied in our preparations after permeabilization of the apical membrane with nystatin and application of a potassium gradient. We found that pretreament with palmatine inhibited a carbachol-activated K^+ current sensitive to ChTX, which blocks basolateral SK4 K^+ channels, and insensitive to 293B, which blocks basolateral KvLQT1 K^+ channels.

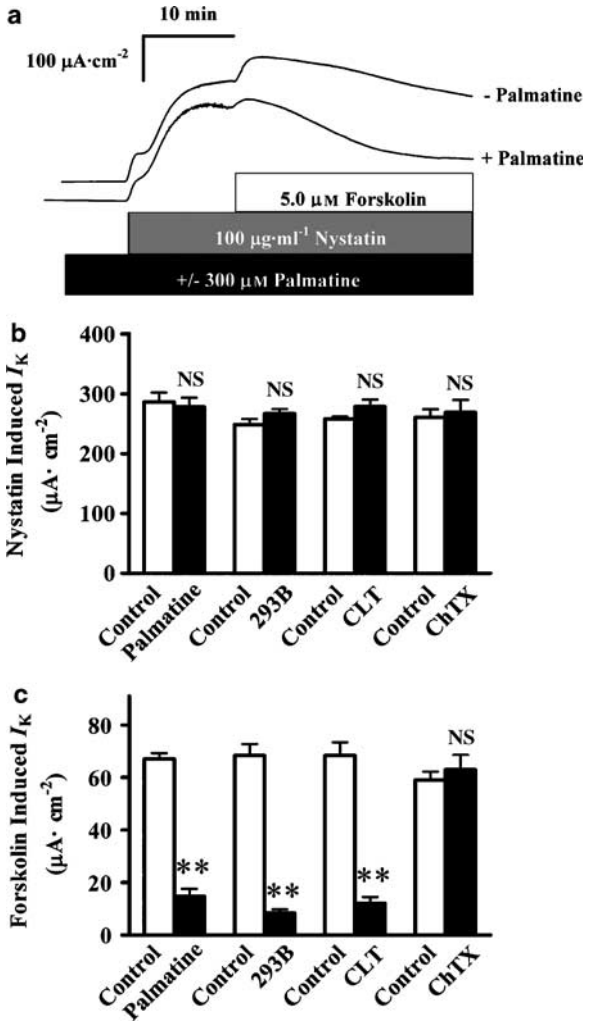

Figure 9 Effect of palmatine on cAMP-dependent I_K across basolateral membrane in isolated rat colonic mucosa. (**a**) Original recordings showing the basal and forskolin-evoked outward I_K pretreated with or without palmatine (300 μM, serosal) in nystatin-permeabilized rat distal colon (100 μg ml^{-1}, mucosal). (**b**) Summarized data showing effect of palmatine and different K^+ blockers in nystatin-permeabilized rat distal colon, palmatine (100 μM, serosal), charybdotoxin (ChTX; 100 nM, serosal), chromanol 293B (293B; 30 μM, serosal) and clotrimazole (CLT; 30 μM, bilateral) were preincubated for 30 min. (**c**) Forskolin (5 μM) was added to the serosal bath 30 min after presence of palmatine and blockers in the same experiments as (**b**). Each column showed as in (**b**) and (**c**) represents mean ± s.e.mean ($n = 6$). $^{**}P < 0.01$, significantly different from the respective controls. NS, not significantly different from the respective controls.

cAMP-activated Cl⁻ secretion

In epithelial cells, sustained Cl^- secretion is generated by raising levels of cAMP, through simultaneous activation of both apical CFTR Cl^- channels and basolateral cAMP-dependent K^+ channels, which are phosphorylated by protein kinase A. Thus, the inhibition by palmatine of forskolin-stimulated sustained Cl^- secretion could involve inhibition of apical CFTR Cl^- channels or inhibition of basolateral K^+ channels (MacVinish *et al*., 2001). Our experiments showed that palmatine attenuated both the apical Cl^- current and the basolateral K^+ current in response to forskolin.

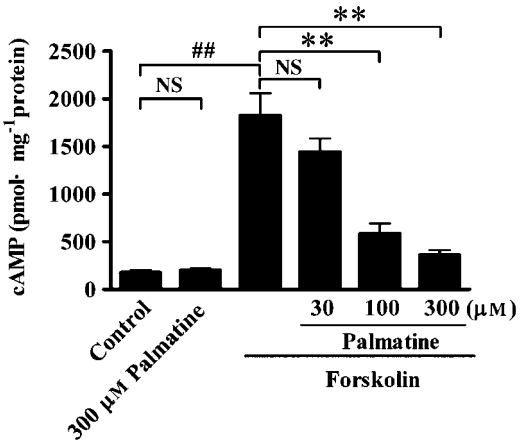

Figure 10 Inhibitory effects of palmatine on the production of intracellular cAMP in rat distal colonic mucosa. The tissues were pretreated with palmatine at concentrations of 30, 100 and 300 μM for 30 min, intracellular cAMP content was determined in rat distal colonic mucosa with or without 5 μM forskolin in the presence of 100 μM isobutylmethylxanthine (IBMX) on both sides for 15 min. Each column represents mean ± s.e.mean ($n = 8–9$). $^{\#\#}P < 0.01$, significantly different from data obtained from control. $^{**}P < 0.01$, significantly different compared with data obtained from forskolin. NS, not significantly different from data obtained from the control or forskolin.

The CFTR is a major Cl^- secretory pathway that regulates the amount of ions and water in the respiratory and colonic epithelia (Pilewski and Frizzell, 1999; Sheppard and Welsh, 1999). To further characterize the apical Cl^- channel in our preparations, we also determined the effects of CFTR inhibitor 172 (a specific CFTR inhibitor), glibenclamide (a nonspecific CFTR inhibitor), NPPB (a CFTR inhibitor) and DIDS (Ca^{2+}-dependent Cl^- channel inhibitor) on forskolin-induced apical Cl^- current. Our results suggested that it was the apical CFTR channel that was the target for palmatine in its actions on the cAMP-mediated Cl^- secretion. However, it is unlikely that palmatine directly inhibits apical CFTR Cl^- channel because palmatine applied to the apical surface was without effect on forskolin-elicited I_{SC}. Our results further demonstrated that palmatine inhibited the basolateral cAMP-sensitive K^+ channel. Basolateral cAMP-activated K^+ channels are predominantly of the KvLQT1 type (Kunzelmann and Mall, 2002). The KvLQT1 (KCNQ1) K^+ channel α-subunit interacts with the β-subunit KCNE3 in the colonic epithelia (Schroeder *et al*., 2000; Dedek and Waldegger, 2001). The K^+ channel activated by forskolin in our experimental system was sensitive to 29B but resistant to ChTX, a profile compatible with the KvLQT1 channel. In our experiments, forskolin did increase cellular cAMP and palmatine inhibited that increase in a concentration-dependent manner. It is therefore most likely that the inhibition of cAMP-activated Cl^- secretion by palmatine is mediated by decrease in intracellular cAMP levels, which then inhibits phosphorylation of protein kinase A, and consequently leads to blockade of the opening of apical CFTR Cl^- channel and inactivation of the basolateral KvLQT1 K^+ channel.

Comparisons with berberine

Our results showed clearly that palmatine inhibited Cl^- secretion in rat colonic mucosa but that the mechanisms involved were critically dependent on the stimulus for that secretion. Secretion stimulated by carbachol or perhaps any other agent capable of raising $[Ca^{2+}]_i$ was inhibited by palmatine through action on the basolateral SK4 K^+ channel, with no apparent effect on apical Cl channels. However, secretion stimulated by raising cellular cAMP levels involved both the apical CFTR Cl^- channel and a different basolateral K^+ channel, KvLQT1.

In contrast to these results, Taylor and his colleagues (Taylor and Baird, 1995; Taylor *et al*., 1999) reported that berberine inhibited Cl^- secretion by blocking of basolateral K^+ channels and was distal to second messenger (cAMP-protein kinase A) production.

Data from present study showed that palmatine inhibits the carbachol-induced Cl^- secretion ($IC_{50} = 24.0 \pm 4.7$ μM) more effectively than the cAMP-induced Cl^- secretion (for PGE_2, $IC_{50} = 61.9 \pm 22.0$ μM; for forskolin, $IC_{50} = 68.7 \pm 19.6$ μM) in isolated rat colonic mucosa. A similar result was observed for berberine on Cl^- secretion in human colonic epithelia and T84 cells (Taylor *et al*., 1999) and in rat isolated rat colon where Cl^- secretion was inhibited by loperamide (Diener *et al*., 1988). However, we also found a differential sensitivity to palmatine in the basolateral K^+ channels with the cAMP-activated K^+ channel being more resistant than the Ca^{2+}-activated K^+ channels (Taylor *et al*., 1999). At present, we do not have an explanation for this phenomenon, which awaits further investigation.

In summary, the major findings of our work are that palmatine attenuated Ca^{2+}-induced Cl^- secretion via blocking the basolateral ChTX-sensitive SK4 K^+ channel, without affecting the apical Ca^{2+}-activated Cl^- channel and reduced cAMP-induced Cl^- secretion by inhibiting both the apical CFTR Cl^- channel and basolateral 293B-sensitive KCNQ1 K^+ channel. These observations that palmatine inhibited increased Cl^- secretion induced by two of the major pathophysiological stimuli (Ca^{2+} and cAMP) suggest that this natural product has considerable potential for development into an agent with wide antidiarrhoeal efficacy. More detailed studies will give us an insight into the antisecretory effects and signalling mechanisms for other protoberberine alkaloids apart from berberine and palmatine.

Acknowledgements

This work was supported by grants from the National Natural Science Foundation of China (30171147), the Project of Modernization of Traditional Chinese Medicine (04DZ19843), Shanghai Science and Technology Committee (Shanghai, PR China) and the E-Institutes of TCM Internal Medicine, Shanghai Municipal Education Commission (E 03008) (Shanghai, PR China). We thank Dr Ka Bian, Department of Integrative biology and Pharmacology, University of Texas-Houston Medical School, for reading and correcting this manuscript. We also thank Professor Yong-Hua Ji, School of Life Science, Shanghai University, for allowing us to perform the Fura-2 experiments in his laboratory.

Conflict of interest

The authors state no conflict of interest.

References

Albano F, de Marco G, Canani RB, Cirillo P, Buccigrossi V, Giannella RA *et al.* (2005). Guanylin and *E. coli* heat-stable enterotoxin induce chloride secretion through direct interaction with basolateral compartment of rat and human colonic cells. *Pediatr Res* **58**: 159–163.

Bleich M, Briel M, Busch AE, Lang HJ, Gerlach U, Gögelein HG *et al.* (1997). K_VLQT channels are inhibited by the K^+ channel blocker 293B. *Pflugers Arch* **434**: 499–501.

Da-Cunha EV, Fechinei IM, Guedes DN, Barbosa-Filho JM, Da Silva MS (2005). Protoberberine alkaloids. *Alkaloids Chem Biol* **62**: 1–75.

Dedek K, Waldegger S (2001). Colocalization of KCNQ1/KCNE channel subunits in the mouse gastrointestinal tract. *Pflugers Arch* **442**: 896–902.

Diener M, Knobloch SF, Rummel W (1988). Action of loperamide on neuronally mediated and Ca^{2+}- or cAMP-mediated secretion in rat colon. *Eur J Pharmacol* **152**: 217–225.

Field M (2003). Intestinal ion transport and the pathophysiology of diarrhea. *J Clin Invest* **111**: 931–943.

Gabriel SE, Davenport SE, Steagall RJ, Vimal V, Carlson T, Rozhon EJ (1999). A novel plant-derived inhibitor of cAMP-mediated fluid and chloride secretion. *Am J Physiol* **276**: G58–G63.

Giri P, Hossain M, Kumar GS (2006). Molecular aspects on the specific interaction of cytotoxic plant alkaloid palmatine to poly (A). *Int J Biol Macromol* **39**: 210–221.

Greger R (2000). Role of CFTR in the colon. *Annu Rev Physiol* **62**: 467–491.

Greger R, Bleich M, Riedemann N, van Driessche W, Ecke D, Warth R (1997). The role of K^+ channels in colonic Cl^- secretion. *Comp Biochem Physiol A Physiol* **118**: 271–275.

Grycová L, Dostál J, Marek R (2007). Quaternary protoberberine alkaloids. *Phytochemistry* **68**: 150–175.

Kunzelmann K, Mall M (2002). Electrolyte transport in the mammalian colon: mechanisms and implications for disease. *Physiol Rev* **82**: 245–289.

Leipziger L, Kerstan D, Nitschke R, Cirillo P, Greger R (1997). ATP increases $[Ca^{2+}]_i$ and ion secretion via a basolateral P2Y-receptor in rat distal colonic mucosa. *Pfluger Arch* **434**: 77–83.

Leung GP, Cheng-Chew SB, Wong PY (2001). Nongenomic effect of testosterone on chloride secretion in cultured rat efferent duct epithelia. *Am J Physiol Cell Physiol* **280**: C1160–C1167.

MacVinish LJ, Guo Y, Dixon AK, Murrell-Lagnado RD, Cuthbert AW (2001). XE991 reveals differences in K^+ channels regulating chloride secretion in murine airway and colonic epithelium. *Mol Pharmacol* **60**: 753–760.

Mall M, Bleich M, Schurlein M, Kuhr J, Seydewitz HH, Brandis M *et al.* (1998). Cholinergic ion secretion in human colon requires coactivation by cAMP. *Am J Physiol* **275**: G1274–G1281.

McNamara B, Winter DC, Cuffe JE, O'Sullivan GC, Harvey BJ (1999). Basolateral K^+ channel involvement in forskolin-activated chloride secretion in human colon. *J Physiol* **519**: 251–260.

Oprins JC, Meijer HP, Groot JA (2000). TNF-α potentiates the ion secretion induced by muscarinic receptor activation in HT29cl.19A cells. *Am J Physiol Cell Physiol* **278**: C463–C472.

Pilewski JM, Frizzell RA (1999). Role of CFTR in airway disease. *Physiol Rev* **79**: S215–S255.

Racková L, Májeková M, Kost'álová D, Stefek M (2004). Antiradical and antioxidant activities of alkaloids isolated from *Mahonia aquifolium*. Structural aspects. *Bioorg Med Chem* **12**: 4709–4715.

Resta-Lenert S, Truong F, Barrett KE, Eckmann L (2001). Inhibition of epithelial chloride secretion by butyrate: role of reduced adenylyl cyclase expression and activity. *Am J Physiol Cell Physiol* **281**: C1837–C1849.

Schroeder BC, Waldegger S, Fehr S, Bleich M, Warth R, Greger R *et al.* (2000). A constitutively open potassium channel formed by KCNQ1 and KCNE3. *Nature* **403**: 196–199.

Schultheiss G, Lán Kocks S, Diener M (2005a). Stimulation of colonic anion secretion by monochloramine: action sites. *Pflugers Arch* **449**: 553–563.

Schultheiss G, Siefjediers A, Diener M (2005b). Muscarinic receptor stimulation activates a Ca^{2+}-dependent Cl^- conductance in rat distal colon. *J Membr Biol* **204**: 117–127.

Sheppard DN, Welsh MJ (1999). Structure and function of the CFTR chloride channel. *Physiol Rev* **79**: S23–S45.

Shin JS, Kim EI, Kai M, Lee MK (2000). Inhibition of dopamine biosynthesis by protoberberine alkaloids in PC12 cells. *Neurochem Res* **25**: 363–368.

Strabel D, Diener M (1995). Evidence against direct activation of chloride secretion by carbachol in the rat distal colon. *Eur J Pharmacol* **274**: 181–191.

Subeki, Matsuura H, Takahashi K, Yamasaki M, Yamato O, Maede Y *et al.* (2005). Antibabesial activity of protoberberine alkaloids and 20-hydroxyecdysone from *Arcangelisia flava* against *Babesia gibsoni* in culture. *J Vet Med Sci* **67**: 223–227.

Suzuki T, Sakai H, Ikari A, Takeguchi N (2000). Inhibition of thromboxane A_2-induced Cl^- secretion by antidiarrhea drug loperamide in isolated rat colon. *J Pharmacol Exp Ther* **295**: 233–238.

Tai YH, Feser JF, Marnane WG, Desjeux JF (1981). Antisecretory effects of berberine in rat ileum. *Am J Physiol* **241**: G253–G258.

Taylor CT, Baird AW (1995). Berberine inhibition of electrogenic ion transport in rat colon. *Br J Pharmacol* **116**: 2667–2672.

Taylor CT, Winter DC, Skelly MM, O'Donoghue DP, O'Sullivan GC, Harvey BJ *et al.* (1999). Berberine inhibits ion transport in human colonic epithelia. *Eur J Pharmacol* **368**: 111–118.

Warth R (2003). Potassium channels in epithelial transport. *Pflugers Arch* **446**: 505–513.

Zhang W, Mannan I, Schulz S, Parkinson SJ, Alekseev AE *et al.* (1999). Interruption of transmembrane signaling as a novel antisecretory strategy to treat enterotoxigenic diarrhea. *FASEB J* **13**: 913–922.